JOURNAL OF SOLID STATE CHEMISTRY 72, 137–144 (1988)

The Electronic Structure of Pyrites, Particularly CuS_2 and $Fe_{1-x}Cu_xSe_2$: An XPS and Mössbauer Study*

J. C. W. FOLMER† AND F. JELLINEK‡

Laboratory of Inorganic Chemistry, Materials Science Centre of the University, Nijenborgh 16, 9747 AG Groningen, The Netherlands

AND G. H. M. CALIS§

Laboratory of Physical Chemistry, Catholic University of Nijmegen, Toernooiveld, 6525 ED Nijmegen, The Netherlands

Received March 3, 1987

The MND skewness of X-ray photospectroscopy (XPS) core levels is used to study the character of the wave functions at the Fermi level of a number of pyrites MS_2 (M = Fe, Co, Ni, Cu). It is shown that the degree of mixing between the metal $3d$ e_g levels with the π^* levels of the S_2 anion is essential in understanding the properties of these materials; while FeS_2 can be described as $Fe^{2+}(S_2)^{2-}$ with Fe^{2+} in the low-spin configuration, CuS_2 is essentially $Cu^+(S_2)^-$. In the pyrite-type solid solutions $Fe_{1-x}Cu_xSe_2$ ($0.4 \leqq x \leqq 0.6$) Cu again has a d^{10} configuration, while Fe retains the spin-paired d^6 configuration, as shown by XPS and Mössbauer spectroscopy.

Introduction

The pyrite phases MS_2 (M = Fe, Co, Ni, Cu, Zn) are often quoted as a suitable system to study the gradual filling of a supposedly quite rigid d band: the $3d$ e_g band. This paper intends to elucidate that for a discussion of these materials the interaction of the $3d$ e_g metal orbitals and the π^* molecular orbitals of the S_2 anion is essential. That this interaction is likely to be strong can easily be seen from the structure. The $3d$ e_g orbitals of the octahedrally coordinated metal extend toward the anion and because the angle M–S–S is about 100°, the π^* orbitals point in the direction of the metal. It will be shown that due to the lowering in energy of $3d$ e_g with increasing atomic number of the metal, a reversal of character of the two bands resulting from the e_g–π^* interaction takes place, such that CuS_2 is essentially $Cu^{1+}(S_2)^{1-}$.

As a consequence, the electronic structure of systems like $Fe_{1-x}Cu_xSe_2$ becomes of interest. It will be shown that, in contrast to comparable systems like the spinel $Fe_{1-x}Cu_xCr_2S_4$, the pyrite system retains a Fe^{2+} low-spin configuration.

* Dedicated to Professor John B. Goodenough on the occasion of his 65th birthday.

† Present address: Dow Chemical, P.O. Box 48, 4530 AA Terneuzen, The Netherlands.

‡ To whom correspondence should be addressed.

§ Present address: D.S.M. Central Laboratory, P.O. Box 18, 6260 MD Geleen, The Netherlands.

0022-4596/88 $3.00

TABLE I
CELL PARAMETERS OF SOME PYRITES

	a (pm)
CuS_2	578.9(1)
$CuSe_2$	611.8(2)
$Ni_{0.8}Cu_{0.2}S_2$	568.7(1)
$Fe_{0.4}Cu_{0.6}Se_2$	599.3(1)
$Fe_{0.5}Cu_{0.5}Se_2$	597.9(1)
$Fe_{0.6}Cu_{0.4}Se_2$	594.2(1)

Experimental

CuS_2 and $CuSe_2$ were prepared in sealed golden capsules embedded in NaCl kept at 400°C and 1.5 GPa for 20 hr. The other preparations were performed in sealed evacuated quartz ampoules from the elements: $Cu_{0.2}Ni_{0.8}S_2$ (650°C, 10 days), $Fe_{1-x}Cu_xSe_2$ (600°C, 1–2 weeks). Although both $FeSe_2$ and $CuSe_2$ are marcasites, mixed pyrites $Fe_{1-x}Cu_xSe_2$ are formed under autogenous circumstances around $x = 0.5$. We obtained homogeneous samples for $0.4 \leqq x \leqq 0.6$ in this way. For values approaching $x = 0$ or $x = 1$, pyrite phases were observed contaminated with $FeSe_2$ (marcasite) or $Cu_{2-x}Se$ and Se. Table I summarizes the lattice parameters of the (homogeneous) samples to which we limit our discussion. The data were obtained using a Guinier–Hägg camera ($CuK\alpha_1$ radiation). In total, the observed lattice parameters ranged from 593.3 to 603.0 pm (approximately corresponding to $x = 0.35$ and $x = 0.8$, respectively). As high-pressure pyrite forms of $FeSe_2$ and $CuSe_2$ do exist, it seems likely that under appropriate pressures and temperatures the synthesis can be extended over the entire range of solid solutions.

The XPS measurements were described before (*1*). Electrical measurements were performed on pressed disks of $Fe_{1-x}Cu_xSe_2$ ($x = 0.4, 0.5, 0.6$) which were sintered with a small excess of Se at ca. 500°C. This procedure was not quite satisfactory. The (four-probe/ac lock-in) resistivity data (ρ) were not entirely reproducible. Seebeck coefficients (α) were measured using two Au blocks as sample holder. Care had to be taken that the amount of helium gas present in the sample chamber was kept constant during measurement, as rather large systematic errors (up to 20%) occurred otherwise. In an absolute sense the data presented may suffer from a systematic error accordingly.

Mössbauer experiments were performed at the Laboratory of Physical Chemistry of the University of Nijmegen. The spectra of $Fe_{0.6}Cu_{0.4}Se_2$ and $Fe_{0.5}Cu_{0.5}Se_2$ were recorded using a 25-mCi source of $^{57}Co/Rh$. Low-temperature spectra were measured using a He-bath cryostat suitable for the application of moderate external magnetic fields parallel to the γ-ray direction.

Results

Figure 1 shows the S $2p$ signals in the XPS spectra of a number of pyrites. Whereas semiconducting FeS_2 and NiS_2 show normal 2 : 1 spin–orbit doublets, metallic $Ni_{0.8}Cu_{0.2}S_2$ and particularly CuS_2 show skew signals. The "tail" of the $2p$ 3/2 component falls under the $2p$ 1/2 peak, thus causing an apparent deviation from the 2 : 1 intensity ratio. The CoS_2 (metallic) signal might be suspected to exhibit some skewness, though much less than CuS_2. In the latter case (and for $Ni_{0.8}Cu_{0.2}S_2$) the skewness can be interpreted as indicating a strong S $3p$ contribution to the partly filled band across the Fermi level (*2*).

It should be noted that the emerging of a tail is accompanied by a shift of the head of the signal toward lower binding energy (cf. NiS_2–$Ni_{0.8}Cu_{0.2}S_2$–CuS_2), probably because the head of the signal corresponds to a final state in which the partly filled band is optimally adjusted to the core hole; this relaxation mechanism is absent in NiS_2.

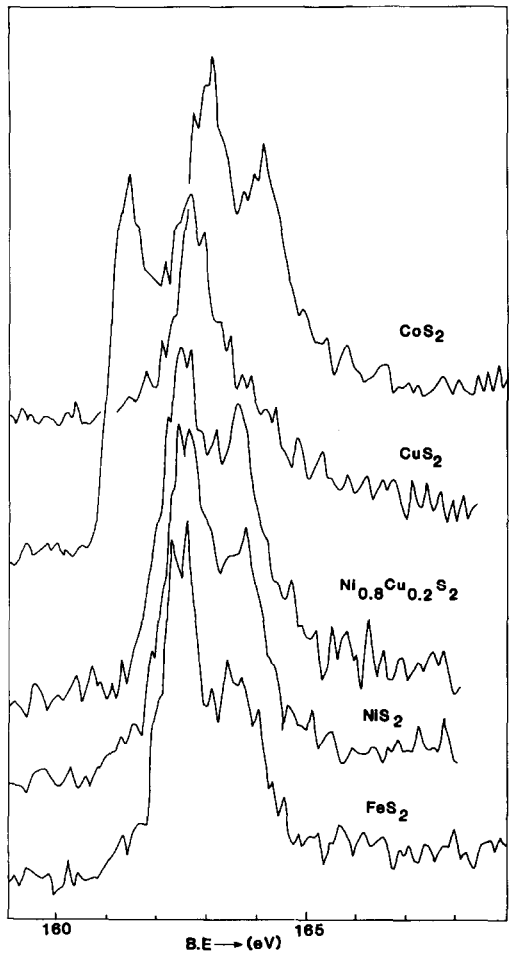

FIG. 1. The XPS S $2p$ signal of some pyrites; monochromatic Al$K\alpha_1$ radiation.

Care should obviously be taken in dealing with chemical shifts of very skew signals.

Figures 2 and 3 show the resistivity (ρ) and Seebeck coefficient (α), respectively, of $Fe_{1-x}Cu_xSe_2$. Although, due to inefficient sintering, the absolute magnitude and slope of ρ are not reliable, the values do indicate rather good metallic conductivity.

This is confirmed by the thermoelectric force (α); calculating values for the slope of α vs T in the expression for metals (assuming impurity scattering) $\alpha = -\pi^2 k^2 T/3eE_F$ we arrive at $E_F = 0.29$, 0.33, and 0.47 eV

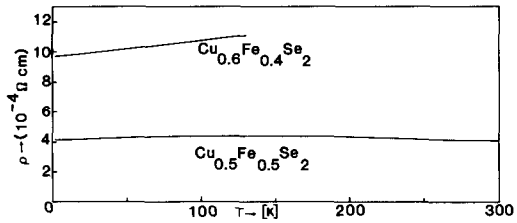

FIG. 2. The resistivity of $Fe_{1-x}Cu_xSe_2$ for $x = 0.5$ and $x = 0.6$.

for $x = 0.4$, 0.5, and 0.6, respectively. This indicates conduction in a rather broad band, e.g., the valence band. Preliminary magnetic measurements indicating Pauli paramagnetic-like behavior support this view.

Figure 4 shows the XPS Fe $2p$ signal of $Fe_{0.5}Cu_{0.5}Se_2$. The rather sharp peak at 706 eV compares well to the spectrum of FeS_2 and indicates a low-spin Fe^{2+} state, so that the compound cannot be $Fe^{3+}Cu^{1+}(Se_2^{2-})_2$. Further details of the spectrum seem mainly governed by the state of the surface. This is not altogether surprising as the low-spin Fe^{2+} state owes its stability to the strong crystal field of six Se_2 pairs. At the surface this type of coordination is not always available for a Fe atom. This may lead to different spin (and/or valence)

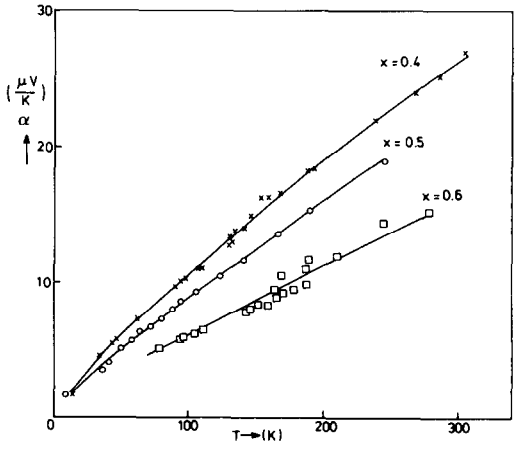

FIG 3. The Seebeck coefficient α of $Fe_{1-x}Cu_xSe_2$ for $x = 0.4$, 0.5, and 0.6; the sign of α is positive.

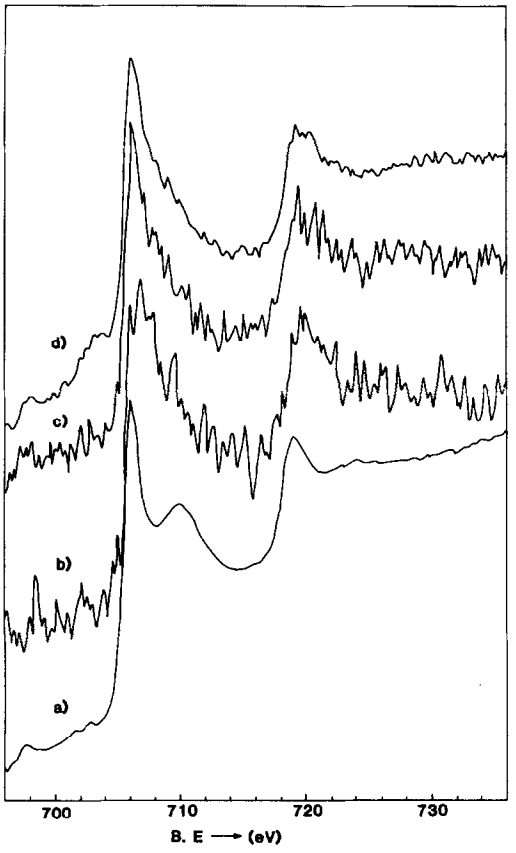

FIG. 4. The XPS Fe 2*p* signal of $Fe_{0.5}Cu_{0.5}Se_2$ initially (a), after 5 min. Ar^+ bombardment (b), and subsequently annealed for 1 hr at 90°C (c), and for 12 hr at 90°C (d). The Ar^+ bombardment made the O 1*s* peak practically vanish.

states which are known to give broad signals around 710 eV. Moreover, the spectra showed a strong sensitivity to small traces of oxygen present in the glove box attached to the X-ray photospectrometer.

The Mössbauer experiments provided more conclusive evidence that the Fe configuration in the bulk indeed remains low-spin Fe^{2+}. Figure 5 shows spectra at room temperature and zero magnetic field. Table II presents the values of the hyperfine parameters obtained from least-squares fits of the observed zero-field spectra. They were fitted with Lorentzian lines, a valid approximation for $\Gamma_{exp} < 0.4$ mm/sec. The spectra recorded at 4.2 K have slightly lower isomer shifts (IS) than the room temperature spectra, due to the temperature dependence of the second-order Doppler shift. The low quadrupole shifts (QS) are nearly temperature independent. This is compatible with high-spin Fe^{3+} with a half-filled *d* band and with low-spin Fe^{2+} with a filled t_{2g} band. Since the iron ions are in approximately octahedral surrounding of Se_2 anions the diamagnetic low spin is more likely in $Fe_{1-x}Cu_xSe_2$. This is further confirmed by spectra recorded in an external magnetic field of 5.2 T (Fig. 6). The solid line in Fig. 6 represents a simulated powder spectrum of diamagnetic Fe^{2+} in $Fe_{0.5}Cu_{0.5}Se_2$, calculated using the zero-field hyperfine parameters given in Table II assuming axial symmetry. The magnetic hyperfine splitting in the spectrum appears to be caused by the external magnetic field only and therefore the spectrum can only be interpreted as originating from a low-spin (diamagnetic) Fe^{2+} configuration.

Discussion

The band structure of FeS_2 is schematically shown in Fig. 7. Calculations of the band structure (*3, 4*) show an appreciable mixing of Fe 3*d* e_g with anion states. The antibonding (e_g, π^*) band, which has 85% e_g character (*3*), is so strongly destabilized

TABLE II

MÖSSBAUER PARAMETERS OF $Fe_{1-x}Cu_xSe_2$

x	*T*	IS	QS	Γ
0.5	298	0.50	0.30	0.33
0.5	4.2	0.45	0.30	0.29
0.4	298	0.49	0.29	0.31
0.4	4.2	0.45	0.33	0.38

Note. Isomer shifts are relative to Fe metal. Temperatures (K), isomer shifts (mm/sec), quadrupole shifts (mm/sec), and widths at half height (mm/sec) are given.

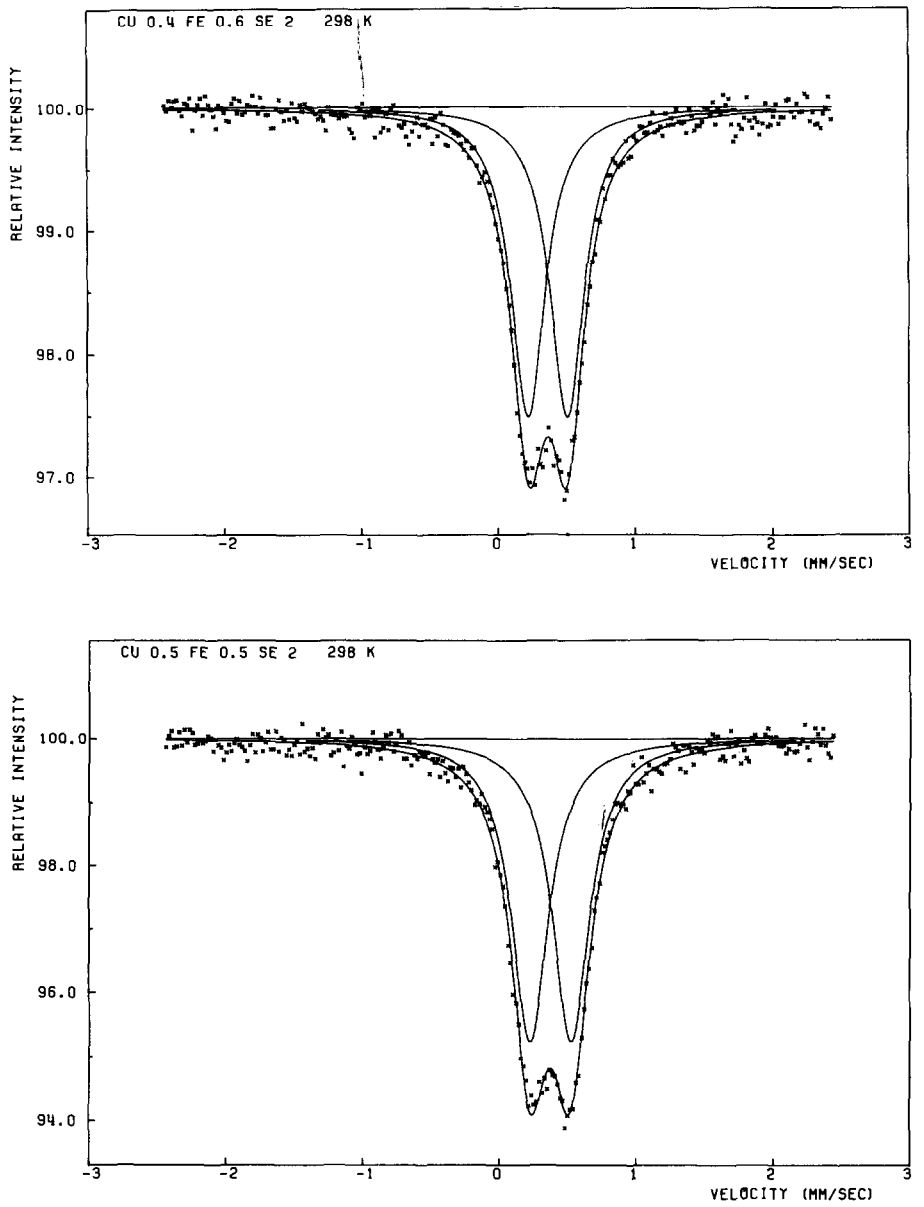

FIG. 5. Mössbauer spectra of $Fe_{1-x}Cu_xSe_2$ for $x = 0.4$ (top) and $x = 0.5$ (bottom) at 298 K without external magnetic field.

in this way that the Fe^{2+} cation adopts the low-spin configuration $t_{2g}^6 e_g^0$. The oxidation state of the S_2 anion is -2.

When going from FeS_2 to CoS_2 and NiS_2, however, the energy of the metal $3d$ orbitals decreases (Fig. 8). Therefore, the bonding (e_g, π^*) band (occupied by four electrons per formula unit) will get more metal character and the antibonding band (occupied by one or two electrons in CoS_2 and NiS_2, respectively) more π^* character. The net result is a decrease of the population of

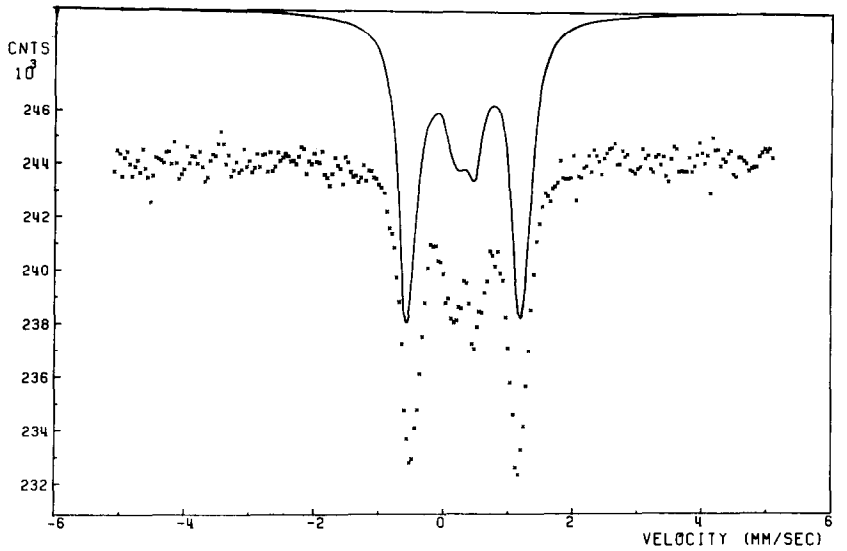

FIG. 6. Mössbauer spectrum of $Fe_{0.5}Cu_{0.5}Se_2$ in an external magnetic field (T = 4.2 K; B = 5.2 T), together with a fit based on a diamagnetic low-spin Fe^{2+} configuration with axial symmetry.

the π^* orbital. This orbital is antibonding with respect to the S–S bond; therefore, the S–S bond becomes stronger, resulting in a decrease of the S–S bond distances and an increase of the separation of the $\sigma(3s)$ and $\sigma^*(3s)$ XPS signals (*5*, *6*) (Table III).

The effect is still more pronounced in CuS_2. Our observations indicate that here the energy of the metal $3d$ orbitals lies below that of the π^* orbital. Therefore, the filled bonding (e_g, π^*) band now is predominantly a metal band, while the partly filled antibonding band has mainly anion character. This means that Cu now has essentially a d^{10} configuration, while the Fermi level lies in an anion band. This is shown by the skewness of the S $2p$ signal and is confirmed by the fact that for the Cu $2p$ XPS signals (*1*, *2*) only a rudimentary satellite and small skewness is observed indicating that the antibonding (π^*, e_g) band

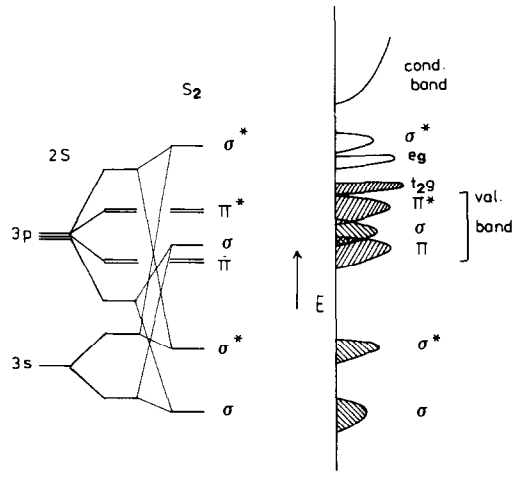

FIG. 7. Molecular-orbital scheme of an S_2 anion and schematical band structure of FeS_2.

TABLE III

THE S–S BOND IN SOME PYRITES

	S–S distance (pm)	BE $\sigma(3s)$–BE $\sigma^*(3s)$ (eV)
FeS_2	218[a]	3.1[c]
CoS_2	213[a]	3.3[c]
NiS_2	206[a]	3.7[c]
CuS_2	203[b]	

[a] Ref. (*7*).
[b] Ref. (*8*).
[c] Ref. (*5*).

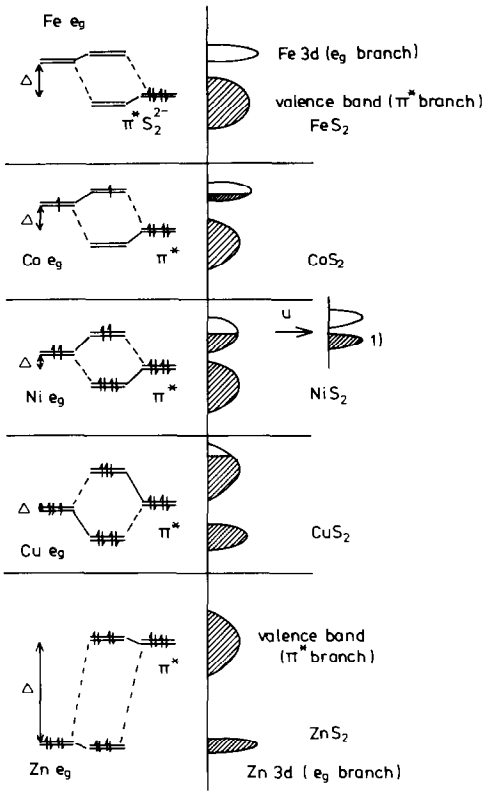

FIG. 8. The interaction between cation $3d$ e_g and anion π^* orbitals (schematic); 1 denotes the splitting of the half-filled e_g band of NiS_2 by the Hubbard U (*4*).

here has indeed little, though still some, metal $3d$ character left. Therefore, the oxidation state of Cu in CuS_2 is +1, that of the S_2 anion −1. In ZnS_2 the $3d$ level already lies at a binding energy of about 10 eV and is generally considered as a core level; both the $3d$ level and the π^* band are completely filled and the anion has the oxidation state −2.

As pointed out, the Cu atoms in CuS_2 are essentially monovalent and have a configuration very close to d^{10} as in all other Cu chalcogenides (*1*). This finding sheds new light on a number of data on Cu pyrites CuX_2 (X = S, Se, Te). The low values of m^* from De Haas–Van Alphen measurements (*9*) can be seen as a proof of the broadening of the antibonding (e_g, π^*) band by its predominant π^* character. The Knight shift (*10*) of Cu can be understood from its d^{10} configuration, and the Knight shifts of Se and Te interpreted as an indication for the presence of holes in the p orbitals of these anions. The superstructure observed in CuS_2 below 130 K (*11*) may indeed result from a differentiation in the S–S bond lengths, if the anomaly is associated with a (partial) removal of degeneracy in the π^* band. The weak ferromagnetic properties of $CuSe_2$ and $CuTe_2$ (*12*) remain unexplained in detail, but the acting of valence-band holes as a strong coupling medium, as found in the spinel $CuCr_2Se_4$ (*13*) and in the solid solutions $TlCu_{2-x}Fe_xSe_2$ ($0 < x < 0.5$) (*14*), indicates that the presence of impurities carrying a magnetic moment in a compound with valence-band holes may lead to partial polarization of the valence-band holes and a coupling of the moments of the impurites. Another implication of the S $3p$ character of the partly filled band in CuS_2 is that the S $3s$ XPS signals, like the S $2p$ ones, are affected by skewness: they are so strongly distorted that we were not able to measure the σ–σ^* distance accurately (Table III).

A further implication of the reversal of character of the (e_g, π^*) bands in CuS_2 is that the resulting antibonding band, i.e., the π^* states of the anion, will undergo destabilization and be lifted toward higher energy compared to an undisturbed situation like ZnS_2. This phenomenon seems general for copper chalcogenides: one could say that the destabilization through the Cu $3d^{10}$ band decreases the effective electronegativity of the chalcogen and makes it behave more like a pnicogen.

This effect may in part be responsible for the results we obtained for the $Fe_{1-x}Cu_xSe_2$ system. If one would take the band structure as schematically shown in Fig. 7 to represent $FeSe_2$, and, in keeping all bands rigid, replace part of Fe^{2+} by Cu^+, thus creating holes, one would expect the va-

lence of the remaining Fe to be affected and turned partly Fe^{3+}. By contrast, our data show that the low-spin Fe^{2+} configuration remains intact and that the holes occur in a broad band, the valence band. This shows that the rigid-band approach is not valid and that it is the π^* branch of the valence band which lies across the Fermi level, not the Fe t_{2g} band.

Acknowledgment

The XPS data on FeS_2, CoS_2, and NiS_2 were kindly placed at our disposal by Dr. H. van der Heide.

References

1. J. C. W. FOLMER AND F. JELLINEK, *J. Less-Common Met.* **76,** 153 (1980).
2. J. C. W. FOLMER AND D. K. G. DE BOER, *Solid State Commun.* **38,** 1135 (1981).
3. M. A. KHAN, *J. Phys. C* **9,** 81 (1976); G. KRILL AND A. AMAMOU, *J. Phys. Chem. Solids* **41,** 531 (1980).
4. W. FOLKERTS, G. A. SAWATZKY, C. HAAS, R. A. DE GROOT, AND F. U. HILLEBRECHT, *J. Phys. C* **20,** 4135 (1987).
5. H. VAN DER HEIDE, R. HEMMEL, C. F. VAN BRUGGEN, AND C. HAAS, *J. Solid State Chem.* **33,** 17 (1980).
6. C. F. VAN BRUGGEN, *Ann. Chim. Fr.* **7,** 171 (1982).
7. G. BROSTIGEN AND A. KJEKSHUS, *Acta Chem. Scand.* **24,** 2993 (1970).
8. H. W. KING AND C. T. PREWITT, *Amer. Miner.* **64,** 1265 (1979).
9. S. M. MARCUS AND T. A. BITHER, *Phys. Lett. A* **32,** 363 (1970).
10. F. GAUTIER, G. KRILL, P. PANNISOD, AND C. ROBERT, *J. Phys. C* **7,** L170 (1974).
11. G. VANDERSCHAEVE AND B. ESCAIG, *Mater. Res. Bull.* **11,** 483 (1976).
12. G. KRILL, P. PANISSOD, M. F. LAPIERRE, F. GAUTIER, C. ROBERT, AND M. NASSR EDDINE, *J. Phys. C* **9,** 1521 (1976).
13. R. P. VAN STAPELE, *In* "Ferromagnetic Materials" (E. P. Wohlfahrt, Ed.), Vol. 3, p. 603, North-Holland, Amsterdam (1982).
14. J. C. W. FOLMER, R. J. HAANGE, AND C. F. VAN BRUGGEN, *Solid State Commun.* **36,** 741 (1980); R. BERGER AND C. F. VAN BRUGGEN, *J. Less-Common Met.* **113,** 291 (1985).